

## RESEARCH ARTICLE

# Effects of Prosthesis Shape and Material on the Contact Mechanics of Elbow Joints Following Radial Head Arthroplasty: An In-Silico Investigation

Faezeh Naghdbishi, MSc; Azadeh Ghouchani, PhD; Farzaneh Safshekan, PhD;  
Kassem Ghayyad, MD; Amir Kachooei, MD, PhD

Research performed at: Faculty of Engineering, University of Isfahan, Isfahan, Iran

Received: 10 January 2025

Accepted: 12 April 2025

## Abstract

**Objectives:** Radial head fractures often require prosthetic replacement, but post-surgical complications like radial neck osteolysis, capitellum osteopenia, and ulnohumeral osteoarthritis can arise due to altered elbow biomechanics. This study used the finite element method to evaluate how radial head prostheses (RHPs) shape and material affect elbow joint biomechanics.

**Methods:** A 3D elbow model was developed, including bones, ligaments, and cartilage. Implants featuring two geometries (anatomical vs. axisymmetric) and three materials (polymethylmethacrylate [PMMA], polyether ether ketone [PEEK], and Cobalt) were tested. Bones were considered isotropic and heterogeneous, ligaments and implants linear elastic, and cartilages were considered hyperplastic materials. Stress distributions, contact stresses, and contact areas were assessed during elbow flexion and forearm rotation.

**Results:** During forearm rotation, Cobalt RHPs exhibited lower stresses in the radial neck, indicating higher stress shielding, and all axisymmetric implants showed increased edge loadings. In rotation, only the PMMA anatomic RHP showed close contact stresses to the intact model, while all other models resulted in lower stress levels. In flexion, anatomical designs produced more uniform stress distributions in the radial neck that resembled intact conditions and matched intact capitellum contact stresses, in contrast to axisymmetric designs. The reduction in the contact area in the ulnohumeral cartilage was most noticeable with all axisymmetric RHPs in flexion.

**Conclusion:** The lower contact areas, higher contact stresses, and lower stresses at the radial neck observed in the presence of most axisymmetric RHPs and anatomic Cobalt RHP can be correlated to postoperative complications. The findings suggest that polymeric anatomical RHPs may be superior to conventional metallic axisymmetric options in preserving elbow biomechanics and reducing postoperative complications. However, their long-term effects need to be further explored.

**Level of evidence:** VI

**Keywords:** Cobalt, Contact mechanics, Finite element method, PEEK, PMMA, Radial head prosthesis

## Introduction

Radial head fractures comprise one-third of elbow fractures, caused by a fall on an outstretched arm or typically resulting from axial and valgus forces or posterior rotational patterns.<sup>1,2</sup> Radial head replacement is performed for displaced and comminuted radial head fractures with disrupted ligamentous stabilizers to restore load transfer and decrease the forces exerted on the

ulnohumeral joint. Aside from the advantages of radial head replacement, some poor outcomes have been reported.<sup>3,4</sup> Different aspects of radial head prostheses (RHPs), such as material and design, including stem length (short or long stem), head design (monoblock or bipolar), head symmetry (axisymmetric vs. nonaxisymmetric), and fixation (loose fit, press-fit or cemented) may affect the

**Corresponding Author:** Azadeh Ghouchani, Department of Biomedical Engineering, Faculty of Engineering, University of Isfahan, Iran

**Email:** a.ghouchani@eng.ui.ac.ir



THE ONLINE VERSION OF THIS ARTICLE  
ABJS.MUMS.AC.IR



normal biomechanics of elbow, joint stability, contact mechanics and kinematics, and implant or cartilage wear which can ultimately contribute to the post-traumatic sequelae.<sup>5</sup>

The first radial head implant of vitalium was introduced in 1941,<sup>6</sup> followed by silastic implants in 1969, which were later abandoned due to unfavorable outcomes.<sup>7</sup> Materials, such as titanium, cobalt-chrome, and stainless steel, were used. However, these materials were associated with relatively fast cartilage wear and neck resorption post-surgery, likely due to their higher stiffness than the adjacent native cartilage and bone.<sup>8</sup> Previous tribological, in vivo, and finite element (FE) studies generally suggest that materials with considerably lower stiffness levels than metals, particularly polymers, can better preserve the opposing articular cartilage and prosthesis's longevity.<sup>8</sup> The most studied polymers are ultra-high-molecular-weight polyethylene, polycarbonate urethane (commercially known as Bionate), and also polyether ether ketone (PEEK),<sup>5</sup> which is widely applied in orthopedic surgery due to its biocompatibility, elastic modulus comparable to the cortical bone, and sterilizability.<sup>9</sup> There are also reports about using biocompatible polymethylmethacrylate (PMMA) bone cement with encouraging results.<sup>10, 11</sup> For instance, antibiotic-impregnated PMMA has been used to make a custom-made radial head prosthesis with promising results and decreased chance of osteolysis and infection.<sup>12</sup> However, the biomechanical performance of PMMA or PEEK-made radial head prostheses has not been thoroughly evaluated. Another crucial aspect of RHP's success is its geometry. While the natural radial head is asymmetric, the most commonly used prostheses for radial head replacement are axisymmetric. With the development of computer-aided modeling, anatomic prostheses have been proposed as alternatives to traditional implants. Several retrospective studies have shown satisfactory short- and mid-term outcomes with anatomic RHPs. However, further research is needed to determine their mechanical superiority over standard RHPs.<sup>13</sup>

In the present study, FE analysis has been used to assess the effect of RHP materials (including metal, i.e., cobalt, PMMA, and PEEK) and geometries (including axisymmetric vs. anatomic designs) on the biomechanics of the elbow joints based on stress distribution, contact stress, and contact area data. The results were compared with the intact joint. The findings of this study can be used to optimize the radial head prosthesis design to improve the outcomes after surgery.

## Materials and Methods

### Three-Dimensional Model Generation

A 25-year-old healthy woman underwent an elbow computed tomography (CT) scan using a clinical scanner (GE Healthcare, Pewaukee, WI, USA) with 140 kV, 80 mAs, 0.5 x 0.5 mm/pixel resolution, and 1 mm slice thickness. The elbow was positioned in extension and full supination

during CT scanning. The CT images in the DICOM format were imported into Mimics (Materialise V.21, Leuven, Belgium) to model a 3D intact elbow joint [Figure 1A].

The elbow bones were segmented based on the bone Hounsfield Unit (HU) threshold [Figure 1B]. Then, the model was transferred to 3-Matic software to smoothen the outer surfaces and convert them to a solid format [Figure 1C]. In this study, the humerus and ulna articular cartilages were modelled with a 0.85 mm thickness<sup>7</sup> in 3-Matic [Figure 1D], which was an average thickness reported in the literature (ranging from 0.19 to 1.73 mm).<sup>14-16</sup>

A copy of the solid model of the bones was introduced into SolidWorks v2015 (SolidWorks® Dassault Systemes, SolidWorks Corp., Waltham, MA, USA) to simulate radial head excision and design the radial head implants. The radial head was cut at the level of the head-neck junction to mimic head excision surgery for implantation [Figure 1E]. Two radial head implant shapes were modeled in this study: 1) anatomic [Figure 1F and 2] axisymmetric [Figure 1G]. Three materials were used for RHPs, including PMMA, PEEK, and Cobalt. The implant models were designed in SolidWorks software based on the intact radial head bone anatomy for the anatomic non-axisymmetric design and the available standard models of the metal radial head prosthesis for the axisymmetric design. The axisymmetric implant head diameter, head height, stem diameter, and stem length were set to be 18, 8.5, 4.5, and 20 mm, respectively, based on the provided data for the Evolve radial head prosthesis (EVOLVE® Modular Radial Head, Wright, Memphis, TN, USA).

The ligaments of the elbow joint were created in Solidworks based on their anatomical landmarks as reference points and added to both intact and implanted 3D models, including medial ulnar collateral ligament anterior bundle (MCLA), medial ulnar collateral ligament posterior bundle (MCLP), proximal radioulnar ligaments connecting the radius and ulna bones [Figure 1H], lateral ulnar collateral ligament (LUCL), and the annular ligament (AL) [Figure 1I].<sup>17</sup>

Non-homogeneous material properties based on local bone density ( $\rho$ ) were assigned to the bones using previously derived equations (Eqs. 1 and 2) for elbow joint bones.<sup>18,19</sup> [Figure 1J].

$$(1) \quad \rho = a + b(\text{HU}) ; a = 527, b = 0.44$$

$$(2) \quad E = 9.354 \times 10^{-7} \rho^{3.15}$$

In these equations,  $a$  and  $b$  are the calibration coefficients,  $\rho$  is the bone density ( $\text{gr}/\text{cm}^3$ ), and  $E$  is Young's modulus (MPa).

Cartilage was considered as a hyperelastic tissue (with a Neo-Hookean strain energy function),<sup>20</sup> while the ligaments, PMMA, PEEK, and Cobalt (metal) were assumed as linear elastic materials, based on previous studies [Table 1].<sup>20-24</sup>

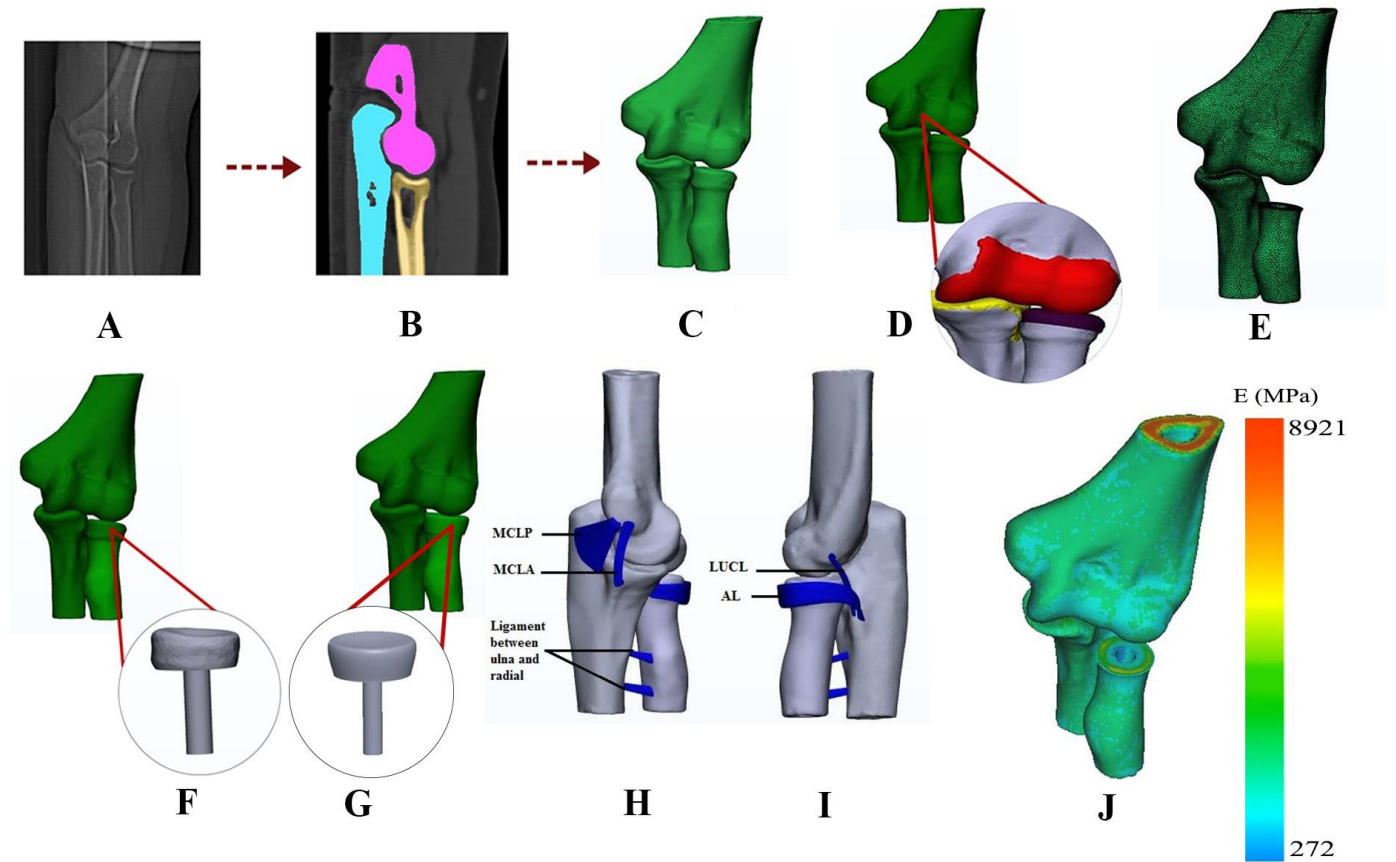


**Figure 1.** Different steps of creating the 3D model of the elbow joint: A) a frontal view of the CT scan images; B) Anterior view of the three masks defined for bones in Mimics; The purple mask shows the humerus, blue mask shows the ulna and yellow mask shows radius mask; C) Anterior view of the 3D model of elbow bones after processing and smoothening the surfaces in the 3-Matic; D) the elbow bones with humerus cartilage (red), ulna cartilage (yellow) and radius cartilage (purple); E) radial head was cut to mimic bone preparation of implantation, then the model was meshed in 3-Matic; F) anatomical PMMA RHP; G) Metal RHP; H) lateral view of the elbow with ligaments I) Medial view of the elbow ligaments, J) 3D model of the elbow joint bones with heterogeneous material properties assigned

**Table 1.** Material properties used for different parts of the FE models

Component	Young's modulus (MPa)	Poisson's ratio	Shear Modulus (MPa)	Bulk Modulus (MPa)
Bone <sup>16,17</sup>	$E = 9.354 \times 10^{-7} \rho^{3.15}$	0.3	-	-
Ligaments (MCLA, MCLP, LUCL, and between ulna and radius) <sup>19</sup>	100	0.4	-	-
Ligament (AL) <sup>20</sup>	250	0.4	-	-
PMMA <sup>21</sup>	1240	0.3	-	-
Cobalt <sup>18</sup>	230000	0.3	-	-
PEEK <sup>22</sup>	4100	0.4	-	-
Cartilage <sup>18</sup>	-	-	0.37	0.31

### Finite Element Analysis

The 3D models were imported into Abaqus (Dassault Systèmes Simulia Corp, V6.14, Providence, RI, USA) for applying boundary conditions and FE analysis. The proximal

end of the humerus was constrained in all degrees of freedom. A reference point (RP) was defined at the end of the radius and coupled to the ulna and radius. Then, a 40°

displacement around the frontal axis (z-axis) was applied to the RP to simulate elbow flexion [Figure 2A]. To model forearm rotation, the ulna was constrained in all degrees of freedom, and the radius was allowed to rotate 80° around its long axis towards the neutral position since the CT scan was

performed in full supination [Figure 2B]. Stress distribution in the models, contact area, and stress during flexion and rotation were studied and compared in the models under investigation, including one intact joint model and the six models containing RHPs.

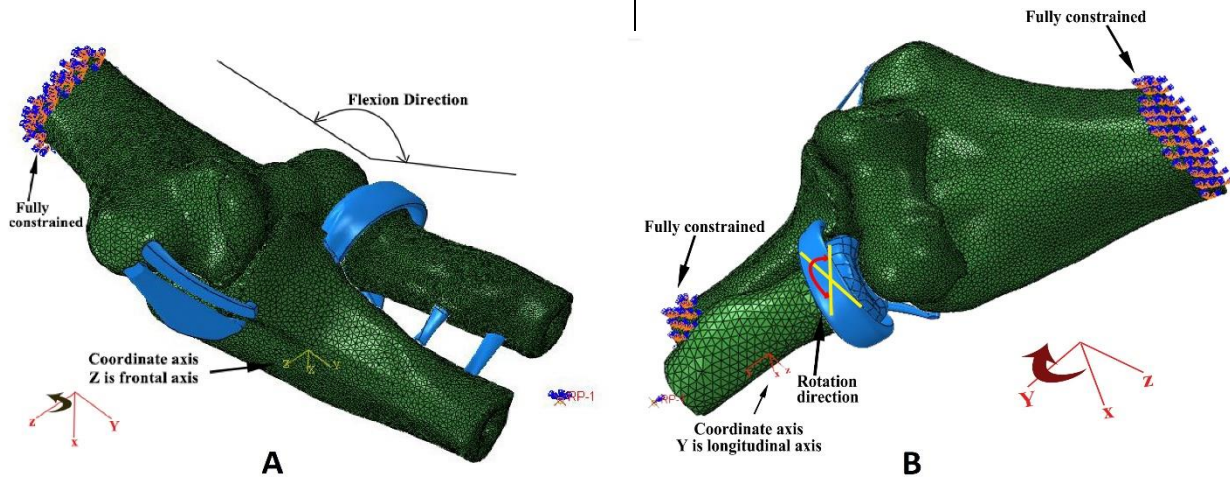


Figure 2. Loading and boundary conditions applied to the models: A) Elbow flexion was simulated by applying a rotation to the RP around the Z axis, which corresponds to the frontal axis; B) Forearm rotation was simulated by applying a rotation to the RP around the Y axis, which corresponds to the longitudinal axis of the bone

## Results

The contact area and maximum contact stress in ulnohumeral, radiocapitellar, and radioulnar articulations and the stress at the radial head were compared between the six implanted models and the intact model during elbow flexion and forearm rotation.

### Contact Stress in Elbow Joints in Flexion Contact Stress on the Capitellum Cartilage

As is shown in [Figure 3A], increasing the flexion angle generally increased the maximum contact stress in the capitellum cartilage in the intact and all implanted models. With increasing flexion angle, the maximum contact stresses on the capitellum cartilage were larger in the presence of axisymmetric implants than in the intact elbow. In contrast,

anatomic implants showed contact stresses relatively closer to the intact elbow. Although the shape of the implants played a great role in the value of the contact stresses, the implant's material had little effect.

### Contact Stress on the Ulnar Cartilage

An increase in the flexion angle increased the contact stress on the ulnar cartilage in all models. In contrast to the capitellum cartilage, at 30° and 40°s of flexion, the maximum contact stress on the ulnohumeral cartilage was larger in the intact elbow than in the implanted models. Still, anatomic implants showed maximum contact stresses relatively closer to the intact elbow, while axisymmetric implants resulted in lower ulnohumeral contact stress [Figure 3B].

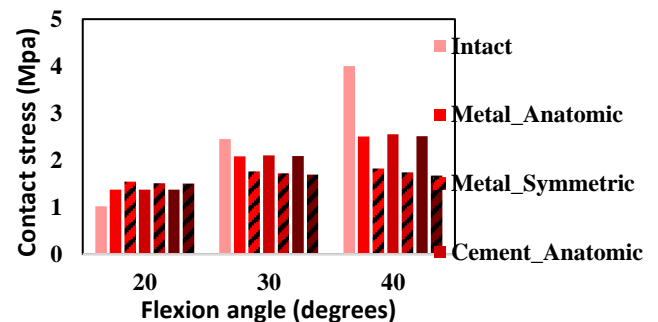
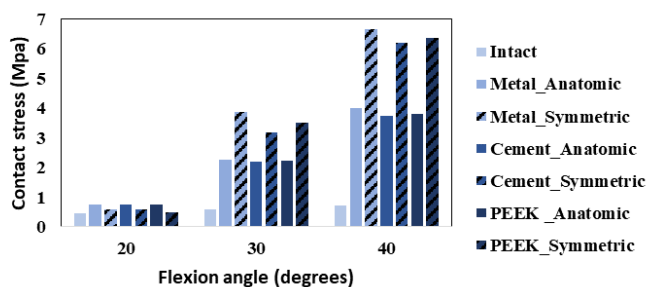


Figure 3. Maximum contact stress values of A) capitellum cartilage B) ulnar cartilage in an intact, Co\_Anat (Metal\_Anatomic), Co\_Sym (Metal\_Symmetric), PMMA\_Anat (PMMA\_Anatomic), PMMA\_Sym (PMMA\_Symmetric), PEEK\_Anat (PEEK\_Anatomic) and PEEK\_Sym (PEEK\_Symmetric) model in flexion



### Contact Area in Elbow Joints in Flexion Contact Area of the Ulnohumeral Joint

In the ulnohumeral joint, increasing the flexion angle increased the contact area in the intact and all implanted models. However, at each flexion angle, the contact area in the intact model was relatively larger (15-19%) than those in the RHP models. The reduction in the contact areas for implanted models is shown in [Figure 4A]. The anatomical-implanted models showed less than a 10 percent reduction in the contact area. In contrast, axisymmetric models showed a 13-19% reduction in the contact area of the ulnohumeral joint compared to the intact elbow. The material of the

implants for both anatomical and axisymmetric implants showed no effect on the contact area of the ulnohumeral joint.

### Contact Area of the Radiocapitellar Joint

Similar to the ulnohumeral joint, the contact area in the radiocapitellar joint was increased with increasing the flexion angle in the intact and all implanted models. However, the contact areas were noticeably smaller in the presence of anatomic and axisymmetric implants than the intact elbow [Figure 4B]. We did not observe any material-related effects on the contact area of the radiocapitellar joint.

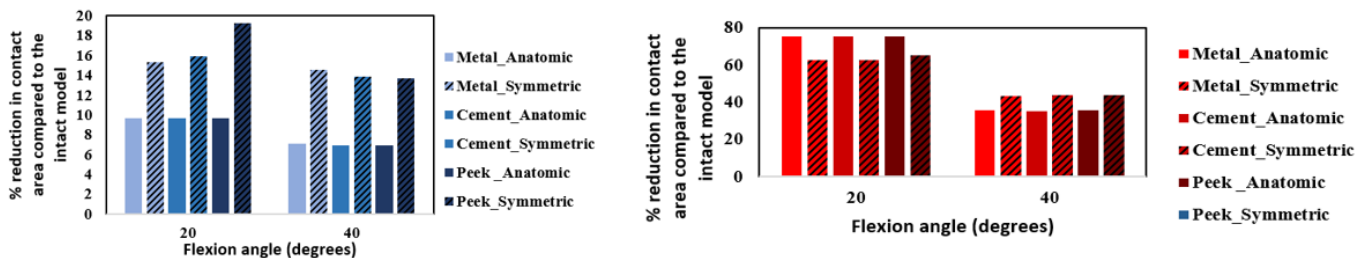


Figure 4. The reduction in the contact area values in percent compared to the intact model in A) ulnohumeral cartilage and B) capitellum cartilage, at 20 and 40° flexion for the intact and implanted models using anatomical and axisymmetric prostheses

### Contact Area of the Radioulnar Joint

In the radioulnar joint, increasing the flexion angle increased the contact area in the healthy model (from 7.24 mm<sup>2</sup> at 20°s to 10.75 mm<sup>2</sup> at 40°s of flexion). However, it almost did not affect the contact area in the implanted models. At all angles, the contact area in the healthy model was greater than the implanted ones. The contact areas of axisymmetric implants (in the range of 5.12 to 5.26 mm<sup>2</sup>) were relatively closer to the intact elbow than those of the anatomic models, which were close to zero.

### Contact Stress in Elbow Joints in Forearm Rotation Contact Stress on the Humerus Cartilage

The maximum contact stress on the humerus cartilage remained almost unchanged for all models during forearm rotation. The maximum contact stresses in the presence of

the anatomic PMMA implant were very close to the intact model, while all other implants led to considerably smaller values [Figure 5A].

### Contact Stress on the Ulnar Cartilage

An increase in the rotational angle increased contact stress on the ulnar cartilage, with its maximum value occurring in the radioulnar region of the cartilage in all models. Axisymmetric implants showed higher stress values than anatomic ones. At 80° of forearm rotation, the contact stresses of all anatomic implants remained similar to or lower than those of the intact model [Figure 5B]. The closest stress values to the intact model (4.96 MPa) were observed in axisymmetric PEEK (4.64 MPa) and Cobalt (4.23 MPa) implants, and the highest stress was observed in axisymmetric PMMA implant (11.6 MPa).

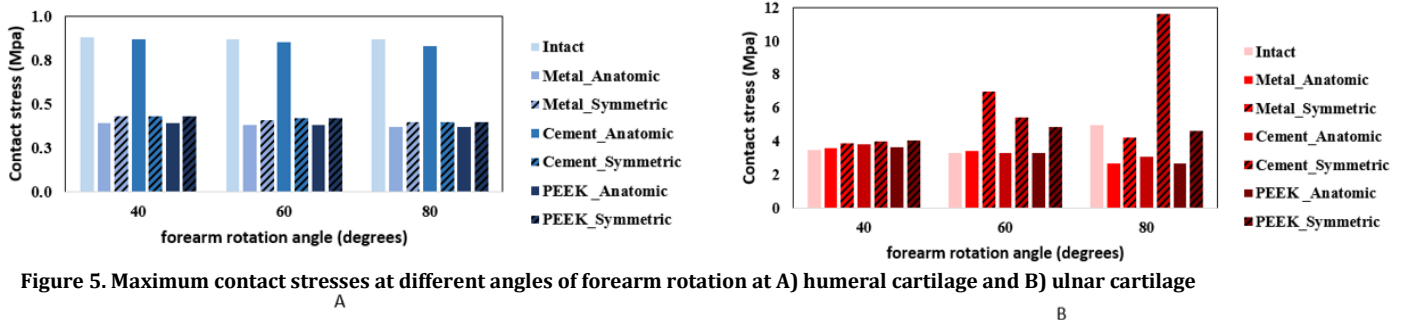


Figure 5. Maximum contact stresses at different angles of forearm rotation at A) humeral cartilage and B) ulnar cartilage

### Contact Area in Elbow Joints in Forearm Rotation

A comparison of contact area among the models during

forearm rotation showed geometry as the most influential factor. However, the amount of change in the contact area in

the presence of the implants was angle and joint-dependent.

#### **Contact Area of the Radiocapitellar Joint**

In the intact radiocapitellar joint, an increase in the rotation angle increased the contact area. We observed no effect of the rotation angle on the contact area in both anatomic and axisymmetric implants, as the contact areas between capitellum cartilage and all implants at all rotation angles equaled zero, which arises from the absence of cartilage thickness on the radial head prosthesis that leads to a gap between the articulating surfaces as mentioned previously.

#### **Contact Area of the Ulnohumeral Joint**

In the ulnohumeral joint, increasing the rotation angle

decreased the contact area in all models. The contact areas of the ulnohumeral joint for all implants at different rotation angles were close to the intact joint, with less than 13% and 5% difference for axisymmetric and anatomic implants, respectively, in 80° rotation [Figure 6]. During forearm rotation in axisymmetric implants, the contact area in the ulnohumeral cartilage was material-dependent. At 40 degrees, the PEEK and PMMA axisymmetric implants led to contact areas very close to the intact model, while cobalt-made RHP led to a larger contact area. All three axisymmetric implants at 80 degrees of rotation also showed a similar contact area to the intact model, while other implants led to slightly higher values.

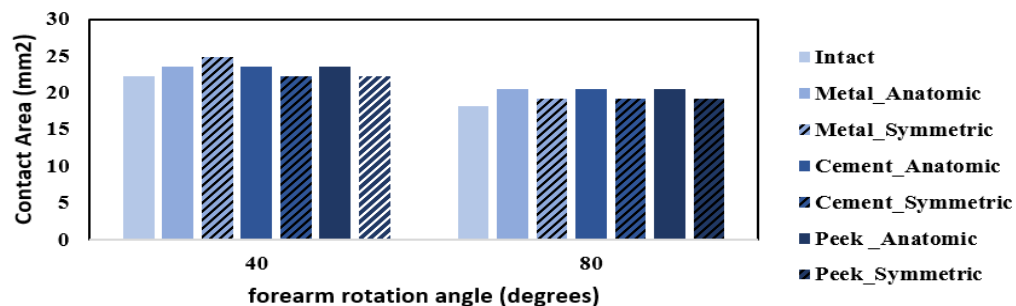


Figure 6. Contact area in ulnohumeral joint at 40° and 80° of rotation

#### **Contact Area of the Radioulnar Joint**

In the radioulnar joint, increasing the rotation angle from 40 to 80° slightly decreased the contact area in the intact model (by as low as 2 mm²). In contrast, it generally increased the contact areas in all other implants. The geometry was the main influential factor, such that at 40° the anatomic and 80°, the axisymmetric implants were closer to the intact joint. At all studied angles, the contact areas in the presence of

axisymmetric implants were least sensitive to the rotation applied, as their corresponding contact areas increased by only about 1 mm² as the angle increased from 40 to 80°, resulting in contact areas smaller than the intact joint. In contrast, anatomic implants were most sensitive to the rotation angle, close to the intact joint at 40°, and considerably larger contact areas were observed at 80° of rotation [Figure 7].

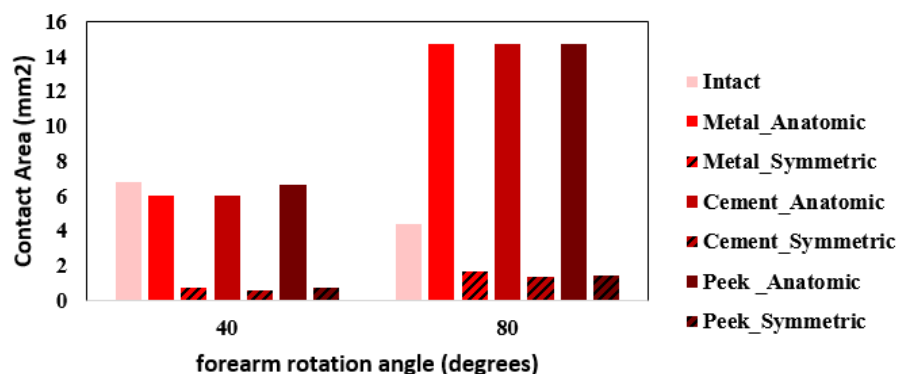


Figure 7. The contact area of the radioulnar joint in different degrees of forearm rotation

#### **Von Mises Stresses in the Elbow joint**

#### **Von Mises Stresses in Elbow Bones in Flexion**

The von Mises stress distribution data in the intact and replaced radial head during flexion were indicative of the

role of the shape and material of the prosthesis on the stress levels. For instance, while the von Mises stress levels in the humerus, ulna, and radius bones increased with increasing the flexion angle in all models, the closest maximum stress values to the intact model (89.3 MPa) at 40° flexion were related to the anatomic and axisymmetric PMMA (93.3 and 93.1 MPa) implants. In comparison, all other models exhibited larger maximum stresses (range: 94.3-94.6 MPa). In the intact model, increasing the flexion angle increased the stress in the trochlea and capitulum, with most of the stress transferring through the ulnotrochlear articulation. In all implanted models, the stress levels in the ulnotrochlear articulation increased with the increase in the flexion angle. The anatomic and axisymmetric implants exhibited higher maximum capitellum stresses than the normal elbow joint. At a 40° flexion angle, the maximum capitellum stress in the

intact model was 0.7 MPa. At the same time, it equaled 2.18 MPa, 2.30 MPa, 2.21 MPa for the anatomic and 3.24 MPa, 3.50 MPa, and 3.31 MPa for the axisymmetric PMMA, metal, and PEEK prostheses, respectively.

#### *Von-Mises Stress in Elbow Bones in Rotation*

In all models, enhancing the rotation angle, similar to the flexion movement, increased the stress levels in the humerus, ulna, and radius bones and demonstrated higher stress levels than the intact model.

The implant shape showed a noticeable impact on the stress distribution in the distal humerus. Anatomic PMMA, axisymmetric PEEK, and metal implants showed the closest stresses to the intact model at 40- and 80-degree rotations [Figure 8].

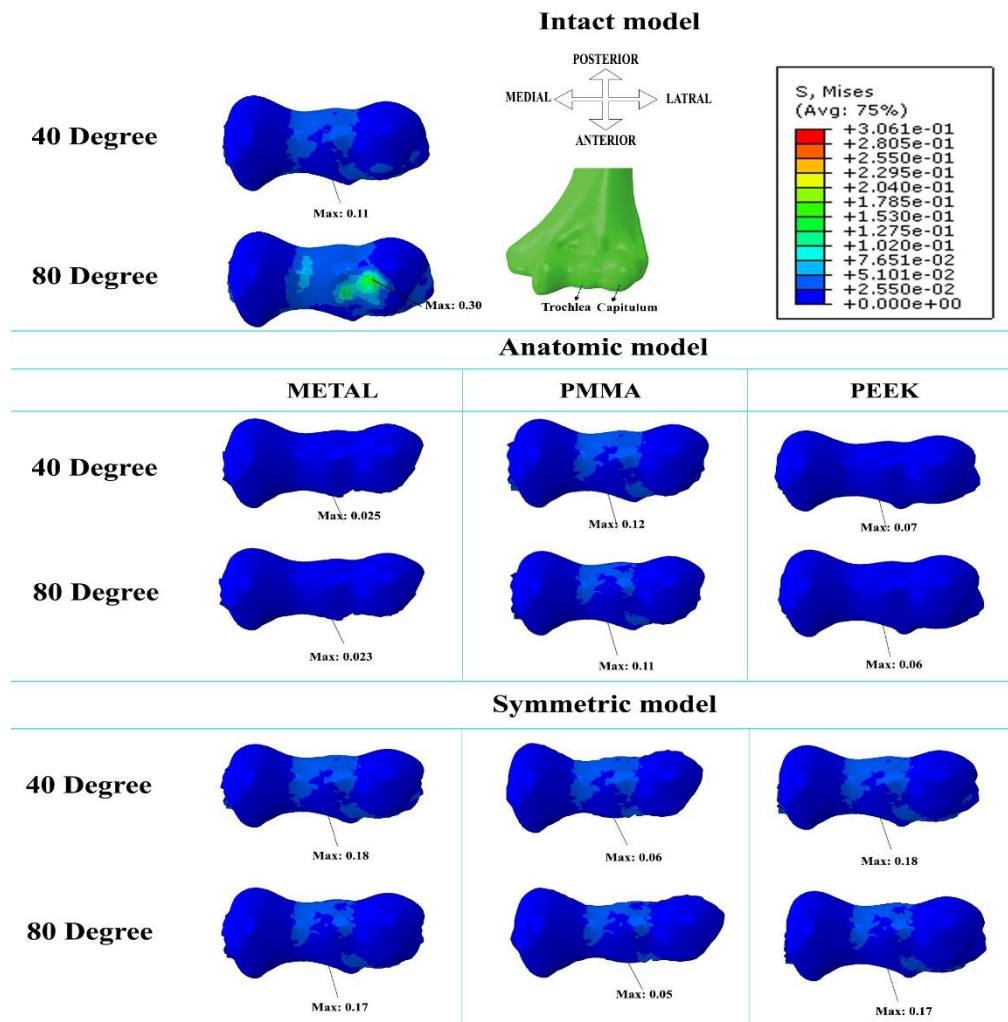


Figure 8. Stress contour on the distal surface of the humerus for intact and implanted models at 40° and 80 ° rotation

**Von-Mises Stress in the Radial Neck and Head in Flexion and Rotation**

In all models, increasing the flexion and rotation angles increased the stress levels in both the radial neck and head. In all implanted models, anatomic implants resulted in lower stresses in the radial head and neck (regardless of the implant material), closer to the intact model.

With increasing the rotation angle, both dish-loading and edge-loading of the intact radial head, indicated by black and red arrows, respectively, in [Figure 9], also increased. Interestingly, the implanted models showed decreased dish-loading and increased edge-loading with the enhancement of

the rotational angle. Despite this, the maximum stresses were lower at the radial head at an 80° rotation in all implanted models than in the intact model. As seen in [Figure 9], the cobalt-made RHPs, regardless of their shape, resulted in much lower stress in the radial neck during forearm rotation. All axisymmetric implants had higher edge loading than their anatomic designs. In flexion, anatomic RHPs showed a more uniform stress distribution in the radial neck. Although the stress was higher at the radial head in all implanted models, lower dish-loading was observed with anatomic implants, thus better resembling the stress distribution on the intact radial head.

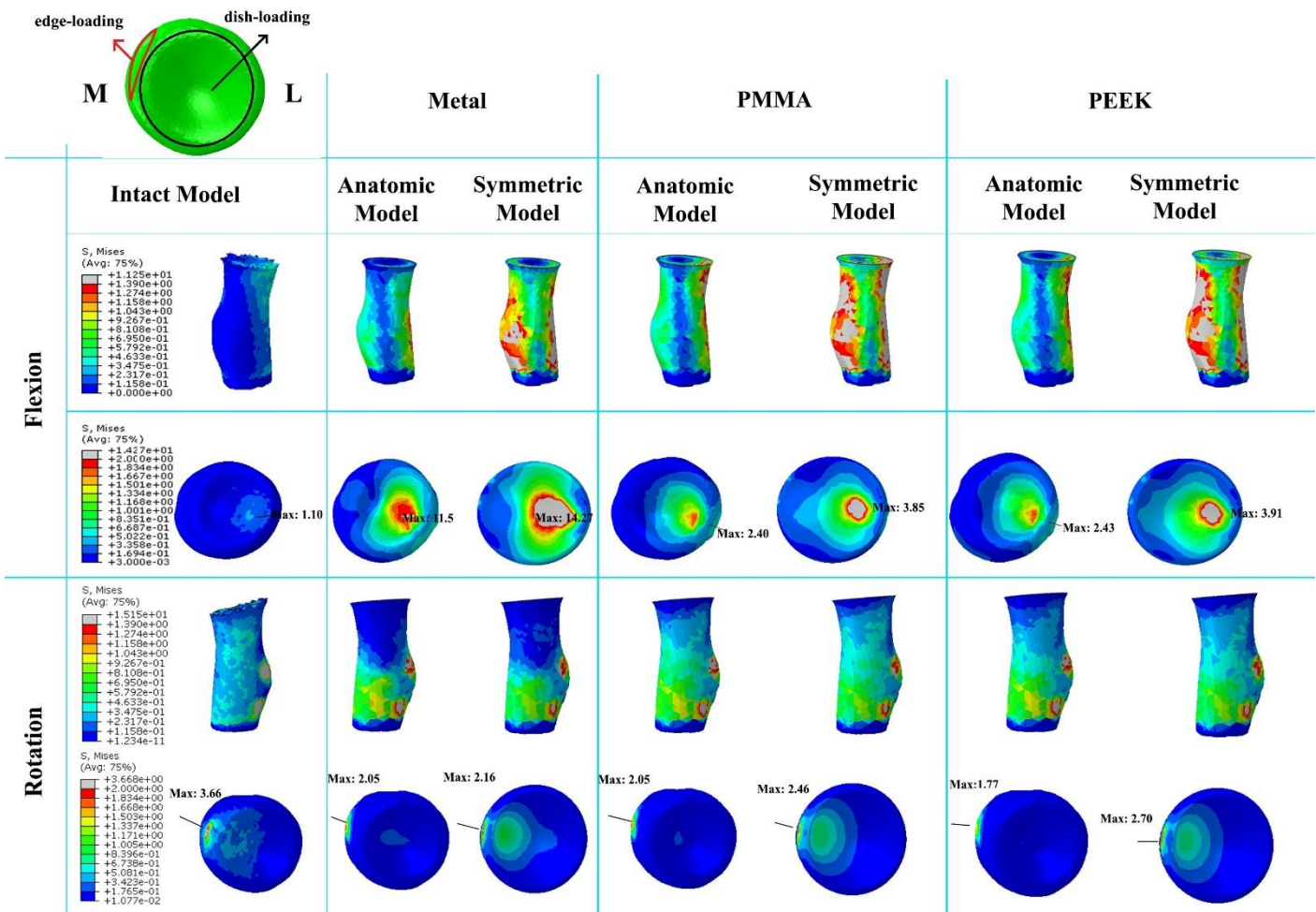


Figure 9. Von Mises stress in radial neck and head for intact and implanted models in 40° of flexion and 80° of rotation

**Discussion**

Elbow hemiarthroplasty is generally presumed to result in reduced joint contact area and increased joint contact stress, leading to cartilage erosion and osteoarthritis pain. These postoperative complications are attributed to weak geometrical consistency and significant stiffness mismatch between the native radial head and the prosthesis, resulting

in abnormal stresses and cartilage softening and degradation.<sup>5</sup> Hence, this study aimed to investigate the effects of the shape and material properties of RHPs on the biomechanics of the elbow joints. The biomechanical performance of anatomical and axisymmetric RHPs made of cobalt, PMMA, and PEEK in forearm rotation and elbow flexion were evaluated and compared with the intact radial



head elbow model using the FE method.

The study's findings highlighted the significant impact of the implant's shape and material on elbow joint biomechanics. The implant's shape had the greatest effect on the contact area of the elbow joints, whereas its material primarily influenced contact stresses, particularly in the radial head. Additionally, the biomechanics of the elbow joints were sometimes dependent on the angle, with no clear pattern observed regarding the implant's stiffening or shape, especially in the von Mises stress of the distal humerus.

Analysis of the contact mechanics of the intact and implanted elbow models during flexion revealed that implant geometry significantly influenced maximum contact stresses and areas. At the same time, the material of the RHPs showed no effect. In the ulnohumeral joint, the anatomic implants were relatively superior at all flexion angles, showing contact areas closer to the intact model. In the radiohumeral joint, differences between the healthy and implanted models were more pronounced and varied with flexion angle; at 20° of flexion, the axisymmetric implants were better, but with increased flexion, the anatomic implants were superior as they led to higher contact areas closer to the intact joint, consistent with Langohr et al.'s findings.<sup>20</sup> In the radioulnar joint, increasing flexion slightly increased the contact area in the intact model but did not affect the implanted models. The axisymmetric implants had larger contact areas like the healthy joint, while anatomic prostheses showed no contact areas. This discrepancy is because the anatomic implants were designed from CT scans that captured the bony regions, excluding the cartilage. This omission may disrupt joint contact. It has been suggested that incorporating a superficial layer to mimic cartilage in the design of anatomical implants could enhance their performance in restoring joint contact mechanics.<sup>20</sup>

In both the humeral and ulnar cartilages, the contact stresses in the presence of anatomic implants were closer to the healthy joint, regardless of the implant material. The presence of radial head implants led to higher contact stresses in the humeral cartilage compared to the intact model, which is consistent with the previously reported data.<sup>20</sup> Still, the intact joint was associated with the highest contact stresses in the ulnar cartilage. In both the humeral and ulnar cartilages, the contact stresses in the presence of anatomic implants were closer to the healthy joint. Such abnormal and higher stresses produced in the joint after surgery, as in the case of axisymmetric implants, can negatively affect the mechanically sensitive cells and cause them to produce enzymes that lead to cartilage softening and degeneration.<sup>5</sup>

Radial neck osteolysis has been reported as a complication following radial head replacement,<sup>25</sup> potentially leading to postoperative fractures. This issue is believed to involve stress shielding effects,<sup>25</sup> which is reported using all types of metallic implants regardless of their fixation method.<sup>26</sup> Our findings on stress distribution just below the RHPs support this hypothesis only for metal implants during forearm rotation, where significantly lower stresses were observed in the radial neck compared to the intact model for anatomic

and axisymmetric implants. However, no such stress reduction, which could lead to bone osteolysis due to stress shielding, was observed in other positions and models. In forearm rotation, the material and shape of the implants influenced the biomechanical data. The maximum contact stresses in the humeral cartilage with the anatomic PMMA implant were very close to those of the intact model. In contrast, all other implants resulted in lower contact stress levels, which may still be acceptable. In the ulnar cartilage, we observed angle- and material-dependent behavior. Anatomic implants produced stresses closer to the intact model, while the highest stresses were seen with axisymmetric implants made of Cobalt and PMMA at 60° and 80° of rotation, respectively. These higher stresses could lead to cartilage wear over time, potentially causing elbow joint pain and reduced range of motion.<sup>27</sup>

A comparison of contact areas during forearm rotation revealed geometry as the most influential factor. However, the changes in the contact area with implants varied depending on the angle and joint. Although a cadaveric study on radiocapitellar joint contact mechanics has shown that anatomic implants provide satisfactory results regarding contact area and pressure,<sup>28</sup> our findings did not show such superior characteristics with anatomic models. In the radiohumeral joint, all implanted models showed zero contact area. It should be attributed to the absence of radial cartilage, which reduces thickness and increases the gap between the radial head and the distal humerus. However, in the radioulnar joint, the contact area was smaller with axisymmetric implants compared to anatomic models. As previously reported, it remained unaffected by the rotation angle due to its geometrical symmetry.<sup>20</sup> This lower contact area can enhance stress, which is thought to increase the risk of long-term joint degradation.<sup>28</sup>

According to the study's findings, the shape of the implant had the greatest impact on the contact mechanics data. In contrast, the implant's material had a greater effect on von Mises stress in certain regions. Previous FE studies by Sahu et al.<sup>29</sup> and Langohr et al.<sup>20</sup> have also emphasized the influence of implant geometry and the orientation of the anatomic implants on the contact mechanics of the radiocapitellar joint. Additionally, research has shown that anatomic radial head prostheses have superior contact mechanics compared to axisymmetric and nonaxisymmetric designs, with increased contact area and decreased contact pressure.<sup>29</sup> An in-vitro study examining the impact of RHP shape demonstrated a significantly lower contact area with axisymmetric prosthesis than quasi-anatomic or patient-specific ones.<sup>30</sup> However, a cadaveric study reported no statistically significant effect of the radial head prosthesis's geometry on the radiocapitellar joint's contact mechanics when using deformable materials like ABS plastic.<sup>29</sup> Due to ABS's minor shape changes under compression, no differences in the contact area were observed among reverse-engineered, quasi-anatomical, and axisymmetric implant designs. The researchers found that all implant shapes (anatomic and axisymmetric) made of ABS resulted in reduced contact areas and elevated contact stresses

compared to a healthy joint when the forearm was rotated from its primary 90°-flexion position.<sup>30,31</sup>

In this study, anatomic implants generally showed better contact mechanics, particularly in the radiohumeral joint or the capitellum stress in elbow flexion and forearm rotation. However, there were some instances where the results were angle-dependent, and these models exhibited inferior contact mechanics compared to the axisymmetric implants. Similarly, Langhor et al.<sup>20</sup> reported that while anatomic implants could improve contact conditions in the radiocapitellar joint in specific rotations and flexions, they could also lead to higher contact stresses and smaller contact areas in some orientations. As a result, axisymmetric implants will remain as better choices, considering their better consistency in rotation.<sup>20</sup>

Regarding von Mises stress data in the intact and implanted models, the anatomic and axisymmetric PMMA and PEEK implants showed stress values closest to the intact models in the radial head during flexion. In rotation, the axisymmetric implants led to closer stress values to the intact model, though the trend was angle-dependent. In the capitellum, the stress was higher in all implanted models. Still, regardless of their material, anatomic implants exhibited closer values to the intact model, reducing the risk of cartilage erosion. A cadaveric study by Chytas et al. reported cartilage loss in the capitulum with metallic monopolar radial head prostheses after 700,000 pronation and supination forearm movements.<sup>27</sup> The material was the most influential factor in the radial head during flexion, with PEEK and PMMA anatomic and axisymmetric implants showing the best results. In contrast, the cobalt implants resulted in considerably higher stresses due to their stiffness. No material effect was observed in this site during rotational movements [Figure 9]. Hence, both the material and the design of the radial head implant affect the progression of the joint's osteoarthritis. The weak geometrical consistency and significant stiffness mismatch between metal axisymmetric radial head prosthesis, which is currently used, and the native cartilage may lead to cartilage erosion and postoperative osteoarthritis.<sup>5</sup> Materials with properties similar to the native radial head are recommended for the ideal radial head replacement.<sup>28</sup> A recent study on the prevalence of osteoarthritis following radial head replacement in 73 patients over 3.4 years revealed a 72% incidence in the humeroulnar and 56% in humeroradial joints.<sup>24</sup> The authors concluded that implant design influences osteoarthritis incidence, with fewer cases in patients with bipolar implants compared with those receiving unipolar implants, likely due to the larger contact area, reducing contact stress at the implant interface.<sup>25</sup>

Lowering the elastic modulus of implants generally improves elbow contact mechanics and prevents cartilage degeneration post radial head implantation, contributing to the long-term success of this procedure.<sup>8,32-35</sup> Dedeker et al. reported that reducing the stiffness of the prosthesis used during hemiarthroplasty results in increased contact area and decreased peak contact stress.<sup>34</sup> Similarly, Berkmortel et al. found that implant material significantly affects contact

area and peak contact pressure on the articulating surfaces.<sup>8</sup> However, the time-dependent behavior of these implants, such as fatigue, creep, stress relaxation, and high-speed loading, should be investigated. Lower stiffness materials like polymers are generally weaker and vulnerable to failure under extreme conditions,<sup>8</sup> raising concerns about their long-term application.

The current FE analysis had some limitations and simplifications. Only the distal humerus, the proximal ulna, and the radius were modeled, excluding full arm motion and muscle forces. The entire elbow bones, shoulder and wrist boundary conditions, and their movements should be considered to achieve a comprehensive stress distribution. The FE models also assumed a constant cartilage thickness, which varies among individuals and is not uniformly distributed over the joint surface,<sup>14</sup> which affects biomechanical results.<sup>35</sup> Herein, forearm rotation, and elbow flexion were simulated, but not supination from the neutral position. Notably, in daily activities, the elbow rarely undergoes supination and typically experiences flexion angles of 15° or more, where it adapts well. Critical conditions and higher stress concentrations are observed in full elbow extension.<sup>36</sup> Pronation results in greater pressure in the humeroradial joint than in supination.<sup>36</sup> Therefore, activities or exercises that involve repetitive pronations and supinations in the full elbow extension or frequent elbow extensions and flexions can lead to abnormal stresses and accelerate cartilage degeneration and osteoarthritis.<sup>36</sup>

## Conclusion

The optimal design of radial head implants is crucial for improving short and long-term postoperative outcomes. Anatomic designs made of less stiff polymeric materials could be considered an alternative to the conventional axisymmetric metallic design, though their long-term effects are still unclear.

## Acknowledgement

N/A

**Authors Contribution:** Authors who conceived and designed the analysis: Azadeh Ghouchani, Amir Kachooi, Faezeh Naghdbishi/ Authors who collected the data: Azadeh Ghouchani, Amir Kachooi, Faezeh Naghdbishi/Authors who contributed data or analysis tools: Azadeh Ghouchani, Amir Kachooi, Faezeh Naghdbishi, Farzaneh Safshekan/Authors who performed the analysis: Azadeh Ghouchani, Faezeh Naghdbishi, Farzaneh Safshekan, Amir Kachooi/Authors who wrote the paper: Azadeh Ghouchani, Amir Kachooi, Faezeh Naghdbishi, Farzaneh Safshekan. Kassem Ghayyad

**Declaration of Conflict of Interest:** The authors do NOT have any potential conflicts of interest for this manuscript.

**Declaration of Funding:** The authors received NO financial support for the preparation, research, and authorship. The fourth author, G. Kassam received financial support for publication of this manuscript.

**Declaration of Ethical Approval for Study:** Ethical approval is not required for this study.

**Declaration of Informed Consent:** Informed consent is not required for this study.

Faezeh Naghdbishi MSc<sup>1</sup>  
Azadeh Ghouchani PhD<sup>1</sup>  
Farzaneh Safshekan PhD<sup>2</sup>  
Kassem Ghayyad MD<sup>3</sup>

Amir R. Kachooei MD, PhD<sup>3</sup>

1 Department of Biomedical Engineering, Faculty of Engineering, University of Isfahan, Iran

2 Department of Mechanical Engineering, Ahrar Institute of Higher Education, Iran

3 Rothman Orthopaedics Florida at AdventHealth, Orlando, USA

## References

1. Ghayyad K, Osbahr DC. Elbow Injuries in Baseball Players: An Orthopedic Perspective. Arch Bone Jt Surg. 2024;12(11):742-745. doi: 10.22038/ABJS.2024.82871.3772. PMID: 39850921; PMCID: PMC11756539.
2. Kaur MN, MacDermid JC, Grewal RR, Stratford PW, Woodhouse LJ. Functional outcomes post-radial head arthroplasty: a systematic review of literature. Shoulder Elbow. 2014; 6(2):108-18. doi: 10.1177/1758573214524934.
3. Grewal R, MacDermid JC, Faber KJ, Drosdowech DS, King GJ. Comminuted radial head fractures treated with a modular metallic radial head arthroplasty: study of outcomes. J Bone Joint Surg Am. 2006; 88(10):2192-200. doi: 10.2106/JBJS.E.00962.
4. Krukhaug Y, Hallan G, Dybvik E, Lie SA, Furnes ON. A survivorship study of 838 total elbow replacements: a report from the Norwegian Arthroplasty Register 1994-2016. J Shoulder Elbow Surg. 2018; 27(2):260-269. doi: 10.1016/j.jse.2017.10.018.
5. Langohr GDG, Willing RT. A narrative review of the biomechanical consequences of prosthesis reconstruction of the elbow. Annals of Joint. 2021; 6
6. Speed K. Ferrule caps for the head of the radius. Surg Gynecol Obstet. 1941; 73:845-850.
7. Kim S. Contact stress analysis of the native radial head and radial head implants. University of Pittsburgh; 2014. 8. Berkmortel C, Langohr GDG, King G, Johnson J. Hemiarthroplasty implants should have very low stiffness to optimize cartilage contact stress. J Orthop Res. 2020; 38(8):1719-1726. doi: 10.1002/jor.24610.
9. Yu Y-H, Liu S-J. Polyetheretherketone for orthopedic applications: A review. Current Opinion in Chemical Engineering. 2021; 32:100687.
10. Capomassi MA, Clembosky GA. Use of a polymethacrylate radial head spacer in temporary reconstruction of complex radial head fracture with associated elbow instability. Tech Hand Up Extrem Surg. 2010; 14(4):252-8. doi: 10.1097/BTH.0b013e3182020d1f.
11. Ghasemi, F., Jahani, A., Moradi, A., Ebrahimzadeh, M. H. and Jirofti, N. (2023). Different Modification Methods of Poly Methyl Methacrylate (PMMA) Bone Cement for Orthopedic Surgery Applications. The Archives of Bone and Joint Surgery, 11(8), 485-492. doi: 10.22038/abjs.2023.71289.3330
12. Maydanshahi MR, Nazarian A, Eygendaal D, Ebrahimzadeh MH, Kachooei AR, Shaegh SAM. 3D printing-assisted fabrication of a patient-specific antibacterial radial head prosthesis with high periprosthetic bone preservation. Biomed Mater. 2021; 16(3). doi: 10.1088/1748-605X/abe217.
13. Samra I, Kwaees TA, Mati W, et al. Anatomic Monopolar Press-fit Radial Head Arthroplasty; High Rate of Loosening at Mid-Term Follow Up. Shoulder Elbow. 2023; 15(2):207-217. doi: 10.1177/17585732221080768.
14. Luenam S, Bantuchai T, Kosiyatrakul A, Chanpoo M, Phakdeewisetkul K, Puncreobutr C. Precision of computed tomography and cartilage-reproducing image reconstruction method in generating digital model for potential use in 3D printing of patient-specific radial head prosthesis: a human cadaver study. 3D Print Med. 2021; 7(1):3. doi: 10.1186/s41205-021-00093-w.
15. Yeung C, Deluce S, Willing R, Johnson M, King GJ, Athwal GS. Regional variations in cartilage thickness of the radial head: implications for prosthesis design. J Hand Surg Am. 2015; 40(12):2364-71.e1. doi: 10.1016/j.jhssa.2015.09.005.
16. Giannicola G, Sedati P, Polimanti D, Cinotti G, Bullitta G. Contribution of cartilage to size and shape of radial head circumference: magnetic resonance imaging analysis of 78 elbows. J Shoulder Elbow Surg. 2016; 25(1):120-6. doi: 10.1016/j.jse.2015.07.003.
17. Kachooei, A. (2025). Discovery of Posterior Oblique Ligament (POL) within the Distal Forearm Cruciate Complex (DFCC). The Archives of Bone and Joint Surgery, 13(3), 134-137. doi: 10.22038/abjs.2025.85035.3872
18. Gupta S, Dan P. Bone geometry and mechanical properties of the human scapula using computed tomography data. Trends in Biomaterials and Artificial Organs. 2004; 17(2):61-71.
19. Khan S, Warkhedkar R, Shyam A. Analysis of Hounsfield unit of human bones for strength evaluation. Procedia Materials Science. 2014; 6:512-519.
20. Langohr GDG, Willing R, Medley JB, King GJ, Johnson JA. Contact analysis of the native radiocapitellar joint compared with axisymmetric and nonaxisymmetric radial head hemiarthroplasty. J Shoulder Elbow Surg. 2015; 24(5):787-95. doi: 10.1016/j.jse.2014.12.011.
21. Goh J, eds. The 15th International Conference on Biomedical Engineering: ICBME 2013, 4th to 7th December 2013, Singapore. Springer Science & Business Media; 2013.

22. Rahman M, Cil A, Bogener JW, Stylianou AP. Lateral collateral ligament deficiency of the elbow joint: A modeling approach. *J Orthop Res.* 2016; 34(9):1645-55. doi: 10.1002/jor.23165.
23. Matuszewski Ł, Olchowik G, Mazurkiewicz T, et al. Biomechanical parameters of the BP-enriched bone cement. *Eur J Orthop Surg Traumatol.* 2014; 24(4):435-41. doi: 10.1007/s00590-013-1230-1.
24. Schwitala A, Abou-Emara M, Spintig T, Lackmann J, Müller W. Finite element analysis of the biomechanical effects of PEEK dental implants on the peri-implant bone. *J Biomech.* 2015; 48(1):1-7. doi: 10.1016/j.jbiomech.2014.11.017.
25. Antoni M, Ginot G, Mereb T, et al. Post-traumatic elbow osteoarthritis after radial head arthroplasty: prevalence and risk factors. *Orthop Traumatol Surg Res.* 2021; 107(2):102814. doi: 10.1016/j.otsr.2021.102814.
26. Chanlalit C, Shukla DR, Fitzsimmons JS, An K-N, O'Driscoll SW. Stress shielding around radial head prostheses. *J Hand Surg Am.* 2012; 37(10):2118-25. doi: 10.1016/j.jhsa.2012.06.020.
27. Chytas I, Antonopoulos C, Cheva A, Givissis P. Capitellar erosion after radial head arthroplasty: a comparative biomechanical study of operated radial head fractures on cadaveric specimens. *Orthop Traumatol Surg Res.* 2018; 104(6):853-857. doi: 10.1016/j.otsr.2018.02.007.
28. Sun Y, Hong H, Adikrishna A, Kim Y-J, Jeon I-H. Contact mechanics of anatomic radial head prosthesis: comparison between native radial head and anatomic radial head prostheses in the dynamic mode. *J Hand Surg Am.* 2019; 44(6):517.e1-517.e7. doi: 10.1016/j.jhsa.2018.08.005.
29. Sahu D, Holmes DM, Fitzsimmons JS, et al. Influence of radial head prosthetic design on radiocapitellar joint contact mechanics. *J Shoulder Elbow Surg.* 2014; 23(4):456-62. doi: 10.1016/j.jse.2013.11.028.
30. Shannon HL, Deluce SR, Lalone EA, Willing R, King GJ, Johnson JA. Effect of radial head implant shape on joint contact area and location during static loading. *J Hand Surg Am.* 2015; 40(4):716-22. doi: 10.1016/j.jhsa.2014.12.017.
31. Lalone EA, Shannon HL, Deluce SR, Giles JW, King GJ, Johnson JA. Effect of radial head implant shape on radiocapitellar joint congruency. *J Hand Surg Am.* 2017; 42(6):476.e1-476.e11. doi: 10.1016/j.jhsa.2017.03.009.
32. Gupta GG, Lucas G, Hahn DL. Biomechanical and computer analysis of radial head prostheses. *J Shoulder Elbow Surg.* 1997; 6(1):37-48. doi: 10.1016/s1058-2746(97)90069-0.
33. Abdullah MR, Goharian A, Abdul Kadir MR, Wahit MU. Biomechanical and bioactivity concepts of polyetheretherketone composites for use in orthopedic implants—a review. *J Biomed Mater Res A.* 2015; 103(11):3689-702. doi: 10.1002/jbm.a.35480.
34. DeDecker S. The efficacy of Bionate as an articulating surface for joint hemiarthroplasty (Master's thesis). The University of Western Ontario (Canada); 2016
35. Willing RT, Lalone EA, Shannon H, Johnson JA, King GJ. Validation of a finite element model of the human elbow for determining cartilage contact mechanics. *J Biomech.* 2013; 46(10):1767-71. doi: 10.1016/j.jbiomech.2013.04.001.
36. Takatori K, Hashizume H, Wake H, Inoue H, Nagayama N. Analysis of stress distribution in the humeroradial joint. *J Orthop Sci.* 2002; 7(6):650-7. doi: 10.1007/s007760200116.
37. Morrey B, An K, Stormont T. Force transmission through the radial head. *J Bone Joint Surg Am.* 1988; 70(2):250-6.